Target Detection Thresholds Using Imaging Spectrometer Data

Donald E. Sabol Jr., John B. Adams,
Milton O. Smith, and Alan R. Gillespie

Department of Geological Sciences
University of Washington, Seattle, Washington

I. Introduction

Detection of target materials in image data has long been of major interest in analysis of image data. Targets (any objects or materials that are being sought in an image) can be detected in multispectral images based on their spatial or spectral properties, or a combination of both. To be detected based on spatial properties alone (e.g.: shape, size, texture), the target must be large relative to image sampling size. In this case, the target must be expressed by a group of pixels. If the multi-pixel target is also spectrally distinct from the background, it can be detected spectrally as well as spatially, which may facilitate identification.

Even though sub-pixel targets cannot be detected spatially, they can be detected spectrally under certain conditions of spectral contrast, spectral sampling, and instrumental noise. The spectrum of a sub-pixel target mixed with the spectrum (or multiple spectra) of the background results in a combined spectral signal. In the context of a multispectral image, where there is spectral variance from pixel to pixel, the target spectrum commonly can be estimated using spectral mixture analysis (e.g.: Adams et al., 1986, 1989; Smith et al., 1990; Gillespie et al., 1990). Thus, spectral mixture analysis can be used to detect and, in some instances, identify targets at the sub-pixel scale.

Many of the conditions that limit the spectral detection of sub-pixel targets have been identified in earlier studies. Siegal and Goetz (1977), for example, observed that the masking effect of vegetation on detection of rocks/soils in a composite spectrum of vegetation and substrate depends upon both the fractions and the spectra of the surface components. In one of the first studies to analyze detectability thresholds, Shipman and Adams (1987) applied two-component spectral mixture models to laboratory spectra to detect small amounts of alunite and kaolinite in desert alluvium. Johnson et al. (in review) used the standard deviation of the difference between the background spectrum and spectral mixtures of the background and target to estimate the threshold for target detection. Because both Shipman and Adams (1987) and Johnson et al. (in review) used laboratory spectra, noise (±1% reflectance), although identified as a limiting factor, was not a major source of error. However, noise can be significant (in excess of ±5% reflectance) in image data, particularity in the narrow bands of hyperspectral systems such as NASA's Airborne Imaging Spectrometer (AIS) and the Airborne Visible-Infrared Imaging Spectrometer (AVIRIS). The effect of different instrumental noise and spectral sampling intervals on spectral abundance was investigated by Goetz and Boardman (1989), who emphasized the importance of spectral contrast between endmember spectra in obtaining accurate fractions, particularly with noisy data.

Equation 1, the general equation for spectral mixture analysis, shows the relationship between the continuum and residuals in detection threshold analysis.

The linear mixing model, used in this paper, comprises linear combinations of component (endmember) spectra:

$$R_{mix,b} = \Sigma (F_{em} \quad R_{em,b}) + E_b \qquad \text{and} \qquad \Sigma F_{em} = 1 \tag{1}$$

where $R_{mix,b}$ is the reflectance of the mixed spectrum at each band (b), $R_{em,b}$ is the reflectance of each endmember (em) at each band, F_{em} is the fraction of each endmember in the scene, and E_b is the residual at each band. If a target is abundant at the sub-pixel scale and distinguishable from the other spectral components throughout the spectrum, it generally can be treated as a spectral endmember. For this case, the detection threshold is the smallest fractional abundance (F_{em}) of the endmember that can be measured above system noise. A procedure for determining this threshold was developed by Sabol et al. (1990) and is referred to as "continuum threshold analysis". However, the target is not normally modeled as an endmember when its sub-pixel abundance is low or when its spectrum deviates from mixtures of the other components at only a few wavelengths (Smith et al. 1985; Gillespie et al., 1990; Adams et al., in press). In this case, the target detection thresholds are best determined by analyzing the deviations of the modeled endmember mixtures from the image data in the band residuals (E_b) using residual threshold analysis (Gillespie et al.; 1990, Roberts et al.; 1990).

In this paper, we present an approach to predict the minimal spectral contribution necessary for detection of a target in the band residuals using residual threshold analysis. This approach was demonstrated for the case of detecting soil in the senescent grassland of the Jasper Ridge, September 1989, AVIRIS data.

II. Residual Threshold Analysis

A target spectrum that can be mimicked by mixtures of the (background) endmembers at all but a few bands may be undetectable using continuum threshold analysis. In this case, the target is detectable in precisely the bands where the endmembers are not well modeled. Using these "diagnostic" bands, threshold detection limits can be determined by residual threshold analysis. Unlike continuum analysis, the target spectrum is not included as an endmember in residual threshold analysis. Consequently, the spectral contribution of the target is partitioned among the endmembers, thereby shifting the computed fractions from the preassigned fractions in the spectral mixture. The partitioning is given by:

$$C_b = \Sigma [F_{em} + (F_t \quad Ft_{em})] R_{em,b} \tag{2}$$

$$\text{and both } \Sigma F_{em} = 1 \text{ and } \Sigma Ft_{em} = 1$$

where C_b is the reflectance of the modeled spectrum (continuum) at each band, F_t is the fraction of the target in the observed mixed spectrum, F_{em} is the fraction of each endmember in the observed spectrum, Ft_{em} is the fraction of the target attributed to each endmember, and $R_{em,b}$ is the reflectance of each endmember at each band. Ft_{em} is determined by spectrally unmixing the target spectrum relative to the endmembers.

To illustrate target detection using continuum threshold analysis, consider a surface composed of three materials that mix spectrally, a target material (covering

50% of the surface) and materials A and B (each covering 25% of the surface). In this example, the spectrum of the target is not included as an endmember. When the mixed spectrum is unmixed relative to the spectra of materials A and B (hereafter referred to as endmembers 1 [EM1] and 2 [EM2]), the fraction of the target spectrum will be partitioned among the endmembers. This partitioning ($\mathbf{Ft}_{em}$) can be determined by spectrally unmixing the target spectrum relative to the endmembers. If, for example, the target is partitioned as .77 endmember 1 and .23 endmember 2, 77% of the target's contribution to the mixed spectrum (50%) will be attributed to endmember 1 thereby shifting the fraction of EM1 to 63% while the fraction of EM2 is shifted to 27%.

In the absence of noise, the target is detected as the residual when the spectrum modeled by the endmembers (Equation 1) is subtracted from the measured spectrum that contains a contribution from the target (Equation 2). In the presence of noise, the fractions of the endmembers may vary in value. The amount of variation in the predicted continuum spectrum can be determined for a given confidence interval by repeatedly combining the predicted continuum spectrum with noise, and unmixing the noisy spectrum. The noise, modeled as having a gaussian distribution about the predicted reflectance at each band, causes the resulting distribution of the apparent fractions to be normally distributed about the initial proportions of the predicted continuum. An example of this distribution is shown in Figure 1 A where a signal-to-noise (SNR) of 50/1 (relative to a 100% reflective target) was used. In this example, the range of uncertainty in the fractions of the predicted continuum due to noise at the 90% confidence interval ranged from 58.9% EM1 and 41.1% EM2 to 67.1% EM1 to 32.9 EM2. The uncertainty in the spectrum of the predicted continuum at the 90% confidence is shown in Figure 1B. Noise also causes a range of uncertainty which also affects the observed spectral mixture ($\mathbf{R}_{mix,b}$ in Equation 1). The target is detectable in the band residuals where the uncertainty due to noise associated with the observed spectrum and predicted continuum do not overlap (Figure 2). In this example, the target is detectable in three wavelength regions: 0.5 to 0.7 μm, 2.02 to 2.2 μm, and 2.25 to 2.4 μm. For any given band, the detection threshold is reached when these uncertainty ranges begin to separate. Therefore, by varying the fractions in the spectral mixture, the detection threshold for each band can be determined.

III. Application to Jasper Ridge Data

The problem of detecting soil in the regions of senescent vegetation on Jasper Ridge, California was used to test residual threshold analysis. This problem was chosen because: 1) the minimal spectral contrast between soil and dry grass makes spectral separation of the two materials difficult (Roberts et al., 1991), and 2) the exposures of soil in the dry grasslands are small and scattered, resulting in spectral mixtures in most image pixels of the grasslands.

To be able to compare predicted detection thresholds that were determined using laboratory spectra (measured in reflectance) to image data (in encoded radiance), the image data were calibrated to reflectance. Two methods were used, the empirical-line calibration and the linear mixing calibration (Roberts et al., 1991). Because the level of noise in an image is an important factor in detecting spectral targets, the noise in the image had to be characterized before any detection analysis could be performed.

A. Evaluation of Noise in Images

We developed a new technique that employs spectral mixture analysis to evaluate image noise. Because noise is measured directly from the image, the instrumental noise is measured at the time of the over-flight. The initial step in determining image noise was to model the image as spectral mixtures of a set of endmembers that account for most of the spectral variation in the scene (low band residuals). For the senescent grasslands in the Jasper Ridge scene, three endmembers were used: "soil 176", "dry grass", and "shade" (Figure 3). The standard deviation was calculated for areas in the image where the band residuals were low (down to the noise level) (STD_b), the assumption being that these residuals contain only noise. Although a portion of the noise is found in the band residuals, the remainder affects the endmember fractions. Therefore, it is necessary to determine how the noise is partitioned between the fractions and residuals. This was determined by constructing a synthetic image composed of a range of spectral mixtures using the laboratory-measured endmember spectra. A known level of noise was added to the image. Then, by inverting the spectral mixing equation, the noisy image was unmixed relative to the endmembers to determine the predicted fractions. Band residuals were determined by subtracting the predicted reflectance from the reflectance observed in the noisy synthetic image. The standard deviation was calculated for each band residual (which contained only noise) as well as for the noise that was added to the image. The fraction of the noise in each band residuals (hereafter referred to as the partitioning coefficient [pc_b]) was determined by dividing the standard deviation of the noise in each band residual by the standard deviation of the noise input into the synthetic image. A plot of the partitioning coefficient for the endmembers used in modeling the AVIRIS scene showed that, on average, 90% of the noise was partitioned into the band residuals while only 10% of the noise caused uncertainty in the fractions (Figure 4).

The total noise in the image ($Noise_{b,Tot}$) was determined by adjusting the standard deviation of the band residuals (STD_b) in the AVIRIS scene for the noise that was partitioned into the fractions by using:

$$Noise_{(b,Tot)} = (1+pc_b)\, STD_b \qquad (3)$$

To cast the apparent image noise into an SNR (relative to a 100% reflectant material), the offsets and gains that were used to calibrate the image to reflectance were used to determine the maximum signal for each band ($R_{b,max}$). The signal-to-noise for each band in the Jasper Ridge AVIRIS image (SNR_b) was determined using:

$$SNR_b = \frac{R_{(b,max)}}{Noise_{(b,Tot)}} \qquad (4)$$

The resulting SNR_b for the Jasper Ridge AVIRIS data (September 1989) is shown in Figure 5.

B. Prediction of Residual Detection Thresholds

Using the procedures discussed above, the residual detection threshold for each band was predicted for the target ("soil 176") in backgrounds composed of "dry grass" and "shade". The results are shown in Figure 6. "Soil 176", which has no distinctive absorption features, was most detectable between 0.5 and 0.6 μm (lowest

detection threshold). Target detectability, which drastically decreased between 1.5 and 1.6 μm (where the threshold was high [> 55%]), improved at longer wavelengths (2.05 to 2.4 μm) where the detection threshold decreased to approximately 20%.

This predicted trend of high detectability at shorter wavelengths, poor detectability between 1.5 and 1.6 μm, and intermediate detectability at longer wavelengths was observed in the band residuals of areas of senescent vegetation on Jasper Ridge when the target ("soil 176") was not included as an endmember.

The bands and thresholds from residual analysis depended upon which endmember was the target. For example, when the grassland was modeled as mixtures of "dry grass" and "shade", "soil 176" (the target) was detected at lower thresholds between 0.5 and 0.75 μm (Figure 7A). However, if the target was "dry vegetation" instead of "soil 176", the grassland (modeled as mixtures of "soil 176" and "shade") would have lower thresholds for target detection at 2.09 μm and 2.27 μm (absorption features caused by cellulose and lignin in "dry grass") (Figure 7B).

IV. Summary and Conclusions

Residual analysis was applied to an AVIRIS image and used to predict spectral detection thresholds of a target in a spectral mixture. The analysis determined which bands were most useful for target detection, even when the target spectrum did not have distinctive absorption features ("soil 176" in the example shown in this paper). Because laboratory measured reflectance values were used, the results from this analysis represent a best possible case for material detection.

The detection problem presented in this paper was selected to demonstrate a method based on spectral mixture analysis to predict target detection thresholds. This method is generally applicable to imaging spectrometer data.

Detection of targets in the band residuals is only one part of spectral mixture analysis. The target may be detected as an endmember (continuum threshold analysis, Sabol et al., 1990) as well as in the band residuals. To determine the lowest detection threshold (highest detectability) of a target in a spectral mixture, both continuum and residual threshold analyses should be performed and compared.

V. References

Adams, J.B., Smith, M.O., and Gillespie, A.R., Simple models for complex natural surfaces: A strategy for the hyperspectral era of remote sensing, Proc. IEEE Intl. Geosci. Remote Sens. Symp. '89, I, 16-21, 1989.

Adams, J.B., Smith, M.O., and Johnson, P.E., Spectral mixture modeling: A new analysis of rock and soil types at the Viking Lander 1 site, J. Geophys. Res., 91, 8098-8122, 1986.

Adams, J.B., Smith, M.O., and Gillespie, A.R., Imaging Spectroscopy: Data analysis and interpretation based on spectral mixture analysis, in Pieters C.M. and Englert P. eds., Remote Geochemical Analysis: Elemental and Mineralogical Composition; LPI and Cambridge Univ. Press, in press.

Gillespie, A.R., Smith, M.O., Adams, J.B., Willis, S.C., Fischer, A.F. III, and Sabol, D.E., Interpretation of residual images: Spectral mixture analysis of AVIRIS images, Owens Valley, California, Proc. 2nd AVIRIS Workshop, Jet Propulsion Laboratory, Pasadena, CA. 4-5 June, JPL Publ. 90-54, 28 pp., 1990.

Goetz, A.F.H. and Boardman, J.W., Quantitative determination of imaging spectrometer specifications based on spectral mixing models, in Proceedings of IGARSS 1989, 1036-1039, 1989.

Johnson, P.E., Singer, R.B., Smith, M.O., and Adams, J.B., Simple algorithms for remote determination of mineral abundances and particle sizes from reflectance spectra, J. Geophys. Res., in revision.

Roberts, D.A., Smith, M.O., Adams, J.B., and Gillespie, A.R., Leaf spectral types, residuals, and canopy shade in an AVIRIS image: AVIRIS, Jet Propulsion Laboratory, Pasadena, CA. 20-24 June, (this volume), 1991.

Roberts, D.A., Smith, M.O., Adams, J.B., Sabol, D.E., Gillespie, A.R., and Willis, S.C., Isolating woody plant material and senescent vegetation from green vegetation in AVIRIS data, Proc. 2nd AVIRIS Workshop, Jet Propulsion Laboratory, Pasadena, CA. 4-5 June, JPL Publ. 90-54, 15 pp., 1990.

Sabol, D.E. Jr., Adams, J.B., and Smith, M.O., Predicting the spectral detectability of surface materials using spectral mixture analysis: Proc.of IGARSS '90 Symposium, 2, 967-970, 1990.

Shipman, H. and Adams, J.B., Detectability of minerals on desert alluvial fans using reflectance spectra, J. Geophys. Res., 92, B10, 10391-10402, 1987.

Siegal, B.S. and Goetz, A.F.H., Effect of vegetation on rock and soil type discrimination, Photogramm. Eng. Remote Sens., 43,191-106, 1977.

Smith ,M.O. and Adams, J.B., Strategy for analyzing mixed pixels in remotely sensed imagery, Proc. NASA/JPL Aircraft SAR Workshop, JPL Publ. 85-39, 47-48, 1985.

Smith ,M.O., Adams, J.B., and Gillespie, A.R., Reference endmembers for spectral mixture analysis, Proc. 5th Australian Remote Sensing Conf., Perth 1990, 331-340, 1990.

VI. ACKNOWLEDGMENTS

We thank Steve Willis for programming assistance. This research was supported by NASA grant NAGW 1319 and a grant from the W.M. Keck Foundation for computer equipment and support.

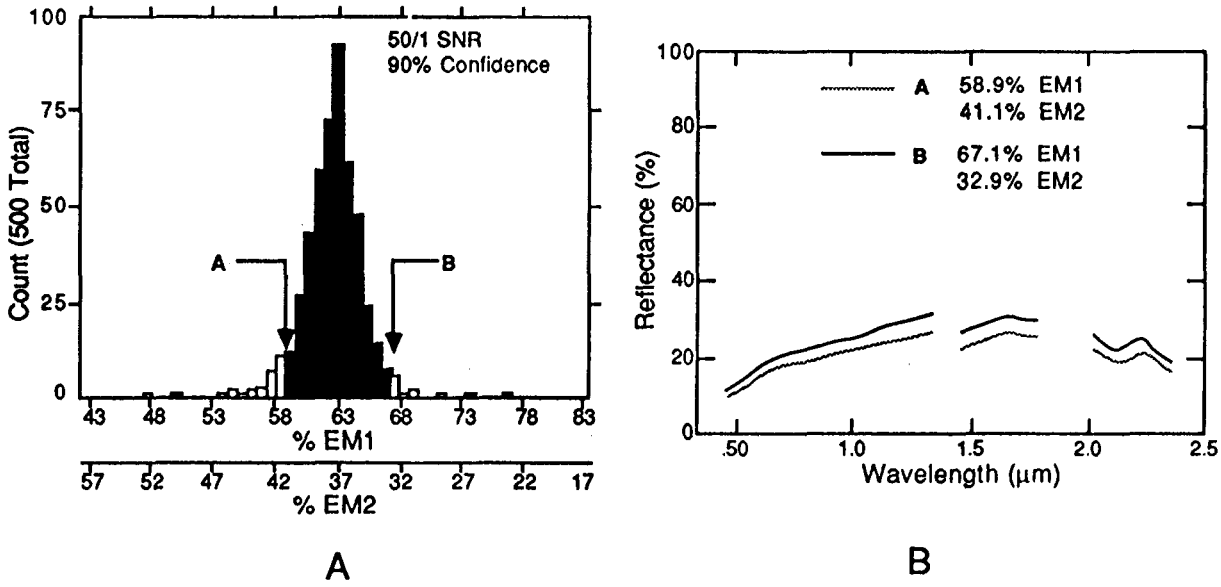

Figure 1. Determination of the uncertainty in the spectrum of the predicted continuum due to noise. For this example, the uncertainty in the fractions of the continuum (mixtures of endmembers 1 and 2) due to a 50/1 SNR at a 90% confidence) range between fractions labeled A and B in Figure 1A. The spectral continuum of these ranges are shown in Figure 1B.

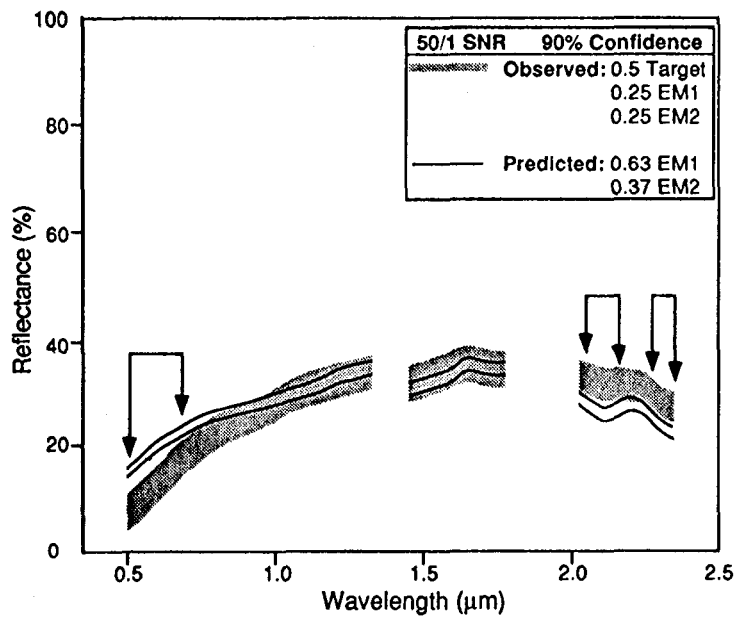

Figure 2. For any band, the target is detectable where the uncertainty due to noise in the predicted continuum (black lines) and the observed mixed spectrum (gray region) do not overlap. In this case, the target is detectable in three wavelength regions: 0.5 to 0.7 μm, 2.02 to 2.2 μm, and 2.25 to 2.4 μm.

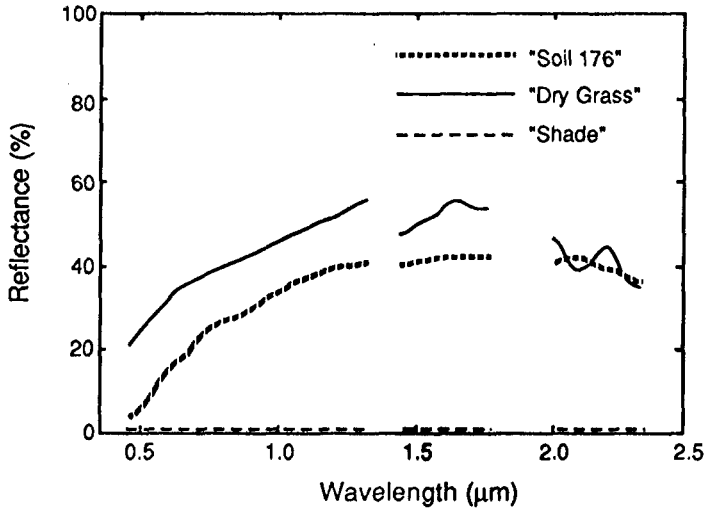

Figure 3. Spectral components observed in the senescent grasslands of Jasper Ridge. "Soil 176" and "dry grass" are laboratory measured spectra that were convolved to the AVIRIS bands used in the spectral analysis. "Shade" was modeled as having 0.1% reflectance at all wavelengths.

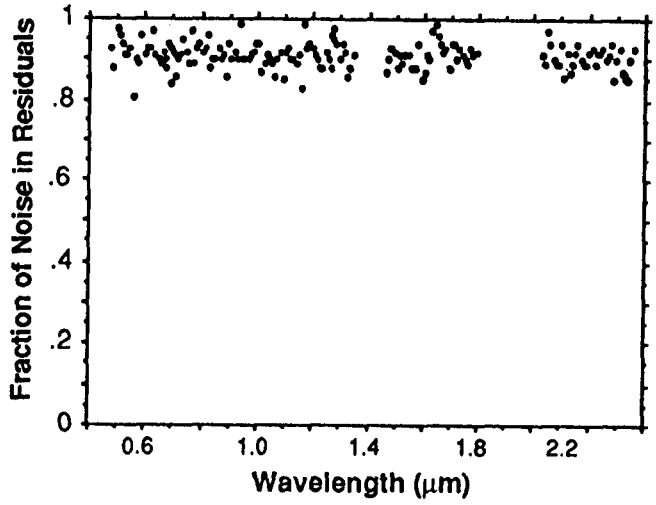

Figure 4. The fraction of the total image noise observed in the band residuals (noise partitioning coefficient) using the spectra shown in Figure 3. On average, 90% of the noise was observed in the band residuals while the remaining 10% affected the fractions.

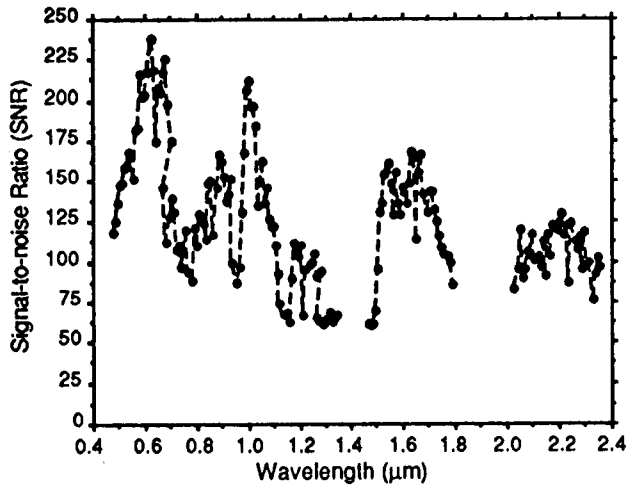

Figure 5. The signal-to-noise ratio (relative to a 100% reflective material) determined from the Jasper Ridge, September 1989, AVIRIS scene.

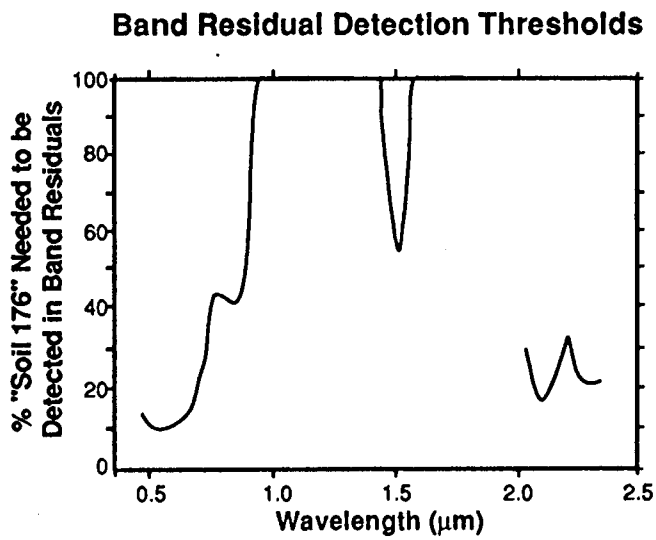

Figure 6. Predicted band residual detectability thresholds for "soil 176" in the areas of senescent vegetation on Jasper Ridge.

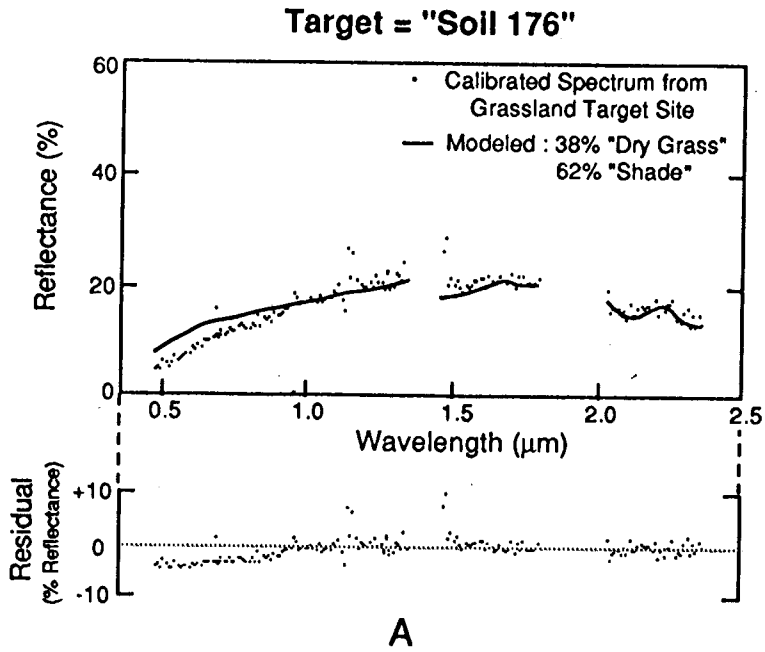

A

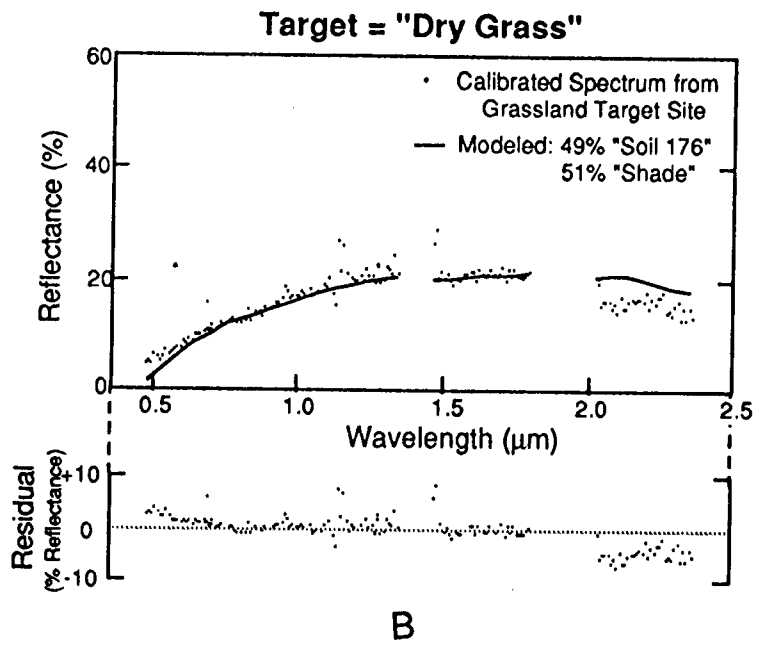

B

Figure 7. The bands in which the target is detectable using residual analysis depend upon which of the component spectra is the target. If the target is "soil 176", the largest band residuals occur at the lower wavelengths (A). However, if the target is "dry grass" the bands in which the target is most easily detected are the higher wavelengths (B).